Available online at www.sciencedirect.com
SCIENCE DIRECT®
Chemical Physics Letters 398 (2004) 505–510
CHEMICAL PHYSICS LETTERS
www.elsevier.com/locate/cplett

In situ fabrication of dispersed, crystalline platinum nanoparticles embedded in carbon nanofibers

Lei Zhang [a], Bin Cheng [b], Edward T. Samulski [a,b,*]

[a] Curriculum in Applied & Materials Sciences, University of North Carolina at Chapel Hill, Chapel Hill, NC 27599-3290, USA
[b] Department of Chemistry, University of North Carolina at Chapel Hill, CB# 3290, Chapel Hill, NC 27599-3290, USA

Received 25 August 2004; in final form 25 August 2004
Available online 18 October 2004

Abstract

Close packed polyacrylonitrile nanofibers containing platinum (II) acetylacetonate were fabricated by polymerization of acrylonitrile in a porous anodic aluminum oxide template. Subsequent pyrolysis results in carbon nanofibers wherein the Pt(II) salt is reduced in situ to elemental Pt. High-resolution transmission electron microscopy showed that the Pt nanoparticles are dispersed throughout the carbon nanofibers, have a size range of 1–4 nm, and are single crystals. Rotating disc electrode voltammetry suggests that the dispersion of Pt nanocrystals in the carbon nanofiber matrix should exhibit excellent electrocatalytic activity.

1. Introduction

To date reported composites containing highly-dispersed platinum particles in carbon nanomaterials are based on rather complicated synthetic procedures [1–4], i.e., fabricating mesoporous carbon nanotubes or foams, introducing a platinum salt (usually H_2PtCl_6) on the porous carbon, then reducing the platinum salt to platinum metal with hydrogen gas [1,2] or by electrodeposition [3,4]. These procedures require considerable platinum salt and involve a multi-step fabrication process that frequently results in aggregated platinum particles which in turn, lowers the available surface area and decreases the mass activity of catalyst. Herein, closed-packed CNFs containing monodispersed platinum nanoparticles (Pt-CNFs) have been prepared by in situ polymerization of acrylonitrile in a porous AAO membrane template, followed by pyrolysis of polyacrylonitrile (PAN) and concomitant reduction of platinum (II) acetylacetonate to platinum metal.

Arrays of carbon nanofibers (CNFs) in a controlled geometry enable the realization of potential applications such as field-emission devices [5] and chemical sensors [6]. Among various nanofabrication techniques, the use of porous anodic aluminum oxide (AAO) membrane templates is one of the easiest and widely applied ways to obtain highly ordered nanomaterials [7–9]. The CNFs fabricated via template synthesis are uniform in diameter, near-hexagonally close packed, perpendicular to the template mold surface [10,11] and in some cases exhibit improved physical properties, e.g., field emission [12]. Furthermore, due to their inherent high surface area, CNFs containing highly dispersed metal nanoparticles are important catalysts [1,2]. For example, the electrocatalytic activity of platinum particles dispersed in carbon nanotubes prepared in mesopores silica templates [1] or AAO membrane templates [2] have been studied. The combination of high surface area with a good dispersion of catalyst is of particular interest in proton exchange membrane fuel cells and direct methanol fuel cells [3].

* Corresponding author. Fax: +1 919 962 2388.
E-mail address: et@unc.edu (E.T. Samulski).

0009-2614/$ - see front matter © 2004 Elsevier B.V. All rights reserved.
doi:10.1016/j.cplett.2004.09.120

The Pt-CNFs were characterized with scanning electron microscopy (SEM), atomic force microscopy (AFM), transmission electron microscopy (TEM), high resolution transmission electron microscopy (HRTEM), and X-ray photoelectron spectroscopy (XPS). We find that single crystalline Pt nanoparticles in the size range of 1–4 nm are highly dispersed in the carbon matrix. The electrocatalytic activity for the reduction of oxygen was determined with rotating disc elelctrode (RDE) voltammetry.

2. Experimental

2.1. Synthesis of Pt-CNFs

Hexagonally packed porous AAO membrane were fabricated by the well-known two-step anodization [13,14] using 0.3 M oxalic acid aqueous solution under a constant voltage of 40 V at 5 °C. Afterwards, the pores were widened by chemical etching in 5% aqueous phosphorous acid at 30 °C. Pt-CNFs were fabricated in the AAO membranes. Fig. 1 shows a schematic diagram outlining the fabrication procedure. AAO templates were immersed in distilled acrylonitrile monomer (CH_3CH_2CN) containing 0.1 wt% 2,2′-azo-*bis*-isobutyronitrile (AIBN) and 1 wt% platinum (II) acetylacetonate [$Pt(acac)_2$]. Polymerization at 50 °C and cyclization at 220 °C were carried out within the AAO templates pores for 10 h, respectively, in air [15]. After removing the residual Al substrate in a mixture of 0.1 M $CuCl_2$ and HCl [16], the PAN nanofibers in AAO membrane were further pyrolyzed at 700 °C [6] under high vacuum for 6 h. Afterwards, the AAO template was dissolved in 6 M NaOH aqueous solution. The Pt-CNFs were cleaned with distilled water, rinsed with ethanol and carefully dried in liquid CO_2 [17] to reduce aggregation of nanofibers induced by solvent surface tension on drying.

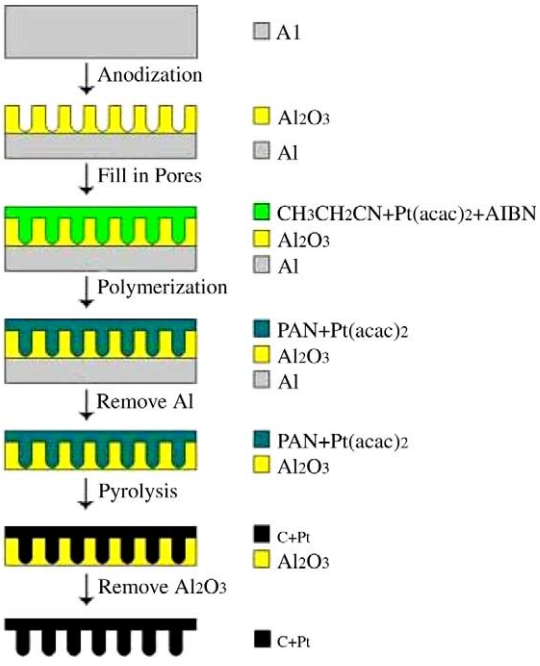

Fig. 1. Schematic diagram of the fabrication of Pt-CNFs using an AAO membrane template.

2.2. Characterization

The surface morphology of the as-prepared AAO membranes was determined by AFM (Nanoscope IIIa). The SEM images of AAO membrane and Pt-CNFs were obtained using JEM6300 microscope. The Pt-CNFs were also examined by TEM (JEM-100CX-II) operated at 100 kV and HRTEM (JEM-2010F-FasTEM) at 200 kV. The XPS measurements of Pt-CNFs were performed on a PHI-5400 spectrometer with a Mg Kα source. The C 1s peak at 284.6 was used as a reference [18,19].

2.3. Preparation of electrodes and electrocatalytic activity measurements

The electrodes were prepared according to reported methods [10]. About 1.0 mg of Pt-CNFs was ultrasonically dispersed in 1.0 ml 5 wt% Nafion and 9.0 ml NANO pure H_2O. Ten μl of the mixture was dropped onto the glassy carbon core (3 mm in diameter). The solvent was slowly evaporated at room temperature over night resulting in a Pt-CNFs-Nafion composite electrode interface (Pt-CNF electrode).

The electrode was mounted in a BAS RDE-1 system with a Platinum counter electrode and a Ag/AgCl (in 3 M NaCl) reference electrode. The electrolyte, 1.0 M H_2SO_4 solution, was purged with either O_2 or Ar before electrocatalytic current measurements at room temperature. The catalytic currents over a range of rotation rates (0–1000 rpm) were recorded at room temperature with a scan rate of 100 mV/s.

For control experiments, electrodes prepared from CNFs without Pt (reaction product from the pyrolysis of polymer from the polymerization of monomer acrylonitrile with 0.1 wt% AIBN in the AAO template) or simply a mixture of Pt-C powder (pyrolysis of bulk polymer prepared from the polymerization of acrylonitrile with 0.1 wt% AIBN and 1 wt% $Pt(acac)_2$ without an AAO template) were used and the results were contrasted with the Pt-CNFs electrode. The three different electrodes are abbreviated as (1) Pt-CNFs, (2) CNFs, and (3) Pt-C. Electrocatalytic currents were measured under the identical conditions with suitable scan ranges.

3. Results and discussion

3.1. Characterization of AAO membranes

Uniform porous AAO membranes were prepared by a two-step anodization. Fig. 2a, the top view of the AAO membranes, indicates that the pore openings on the surface are closed-packed with ~80 nm diameters. Fig. 2b is a cross-sectional view of the AAO membrane showing that all of the nanopore channels are reasonably straight, parallel and traverse the entire thickness of the membrane. The two-dimensional (Fig. 2c) and three-dimensional (Fig. 2d) AFM height images show the surface morphology of AAO membranes to consist of periodically arranged pores (interpore distance of 119 nm) and randomly distributed protuberances as high as 50 nm.

3.2. Characterization of Pt-CNFs

The morphologies and composition of Pt-CNFs were investigated by SEM, TEM, HRTEM and XPS. Fig. 3a is a SEM image of the Pt-CNFs that illustrates uniform nanofibers which are straight and parallel to each other, and hexagonally close-packed. The TEM image of the specimen is shown in Fig. 3b. The diameters of the nanofibers are nearly 80 nm, which is in agreement with the pore diameter of the AAO template. The lengths of the nanofibers are determined by the thickness of the AAO template. The upper-right inset in Fig. 3b shows a selected area electron diffraction (SAED) pattern. The rings correspond to the diffraction from the (1 1 1), (2 0 0), (2 2 0) and (3 1 1) planes of crystalline Pt particles. Fig. 3c, the HRTEM image of Pt-CNFs, indicates that the Pt nanoparticles embedded in amorphous carbon matrix are perfectly crystalline and highly dispersed. The upper-right inset in Fig. 3c is a higher magnification image showing a single Pt nanocrystal with its (1 1 1) and (1 1 1) plane orientations at an angle of 70.5°. The interplane distance (0.23 nm) corresponds to the distance between two adjacent (1 1 1) planes. The size of the Pt nanoparticles in CNFs maxtrix are narrowly distributed as shown in Fig. 3d. Based on measurements of more than 150 nanoparticles, the mean particle size is 2.2 nm; over 70% are between 1.5 and 2.5 nm.

The formation procedure of the Pt nanoparticles is proposed to occur as follows: As the polymerization proceeds, the medium becomes more viscous and the solvent quality of the polymer-rich solution (relative to the monomer) probably decreases. As a result, the $Pt(acac)_2$ molecules probably begin to aggregate/precipitate from solution forming platinum-rich domains within the solidifying polymer matrix. Finally these domains of platinum salt decompose with minimal diffusion during

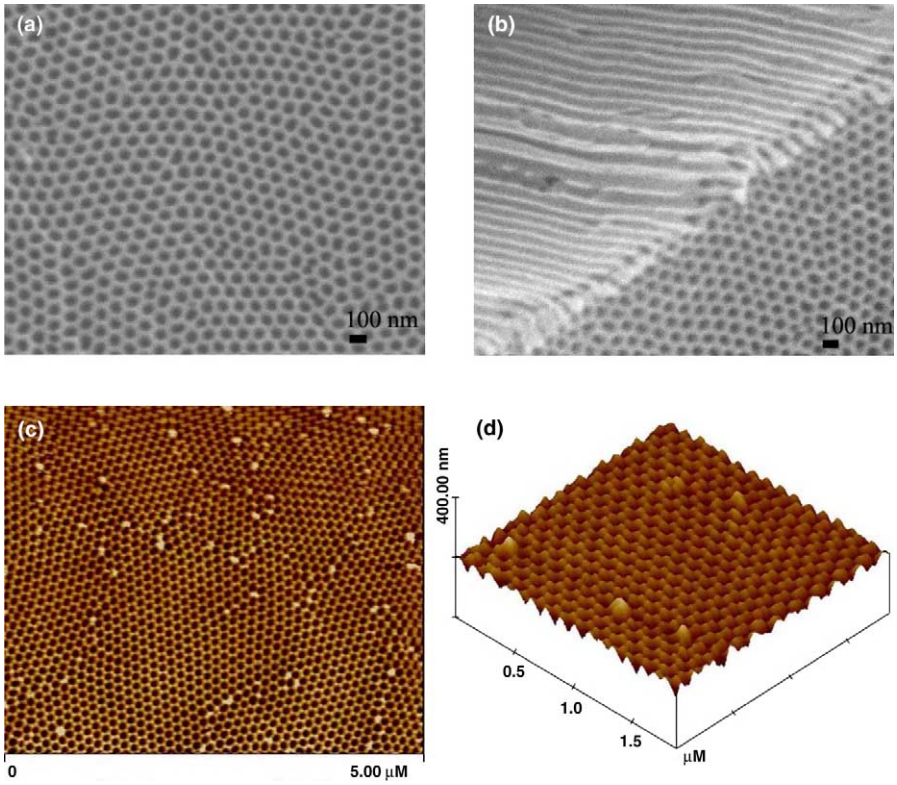

Fig. 2. SEM micrographs of (a) top and (b) cross-sectional views of AAO membranes. Two-dimensional (c), three-dimensional (d) AFM height images of AAO membranes.

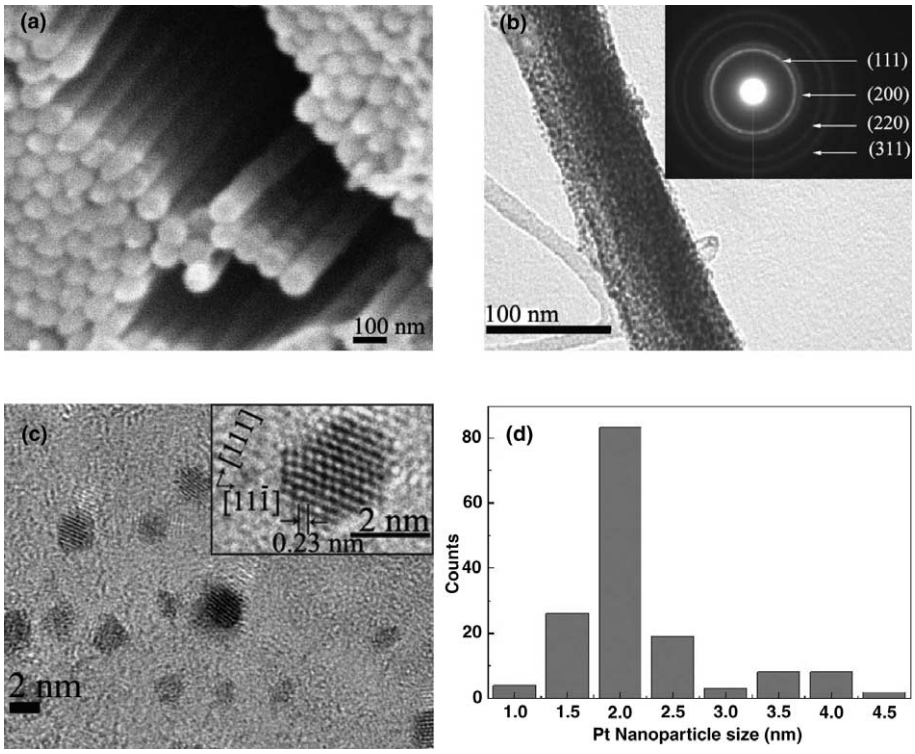

Fig. 3. (a) SEM image of the Pt-CNFs; (b) TEM image of a selected area of Pt-CNFs; the upper-right inset is a selected area electron diffraction pattern showing the diffraction rings coming from Pt nanoparticles; (c) HRTEM image of the Pt-CNFs; the upper-right inset is a larger magnification image showing the (1 1 1) and (1 1 −1) plane orientations of cubic, single-crystalline Pt nanoparticle; (d) the size distribution of the embedded Pt nanoparticles.

the pyrolysis of PAN nanofibers. Moreover the Pt salt is reduced to elemental platinum during the pyrolisis. As a result, Pt nanoparticles are isolated and immobilized in the carbonaceous matrix unable to diffuse and coalesce during pyrolisis [20].

The oxidation states of the composition elements in Pt-CNFs were determined by XPS. Fig. 4a shows the survey scan for the specimen, which consists of four peaks, C 1s, O 1s, Pt 3d, and Pt 4f. Unlike reported data [19], the N peak is barely visible in the survey XPS spectrum; this may be due to the pyrolysis in high vaccum in contrast to reported studies with pyrolysis under an argon atmosphere. Fig. 4b–d show XPS multiplex scans for the C 1s, O 1s and Pt 4f regions, respectively. The C 1s signal could be deconvoluted into carbon peaks in two kinds of chemical environments, the graphitic carbon at 284.6 eV and C–O or C═O species at 286.3 eV [18,19]. The oxygen peak at 532.1 eV may also correspond to O═C and O–C species [19]. The Pt 4f signals could be decomposed into two pairs of doublets. The intense peaks centered at 71.1 and 74.4 eV, respectively, belong to Pt $4f_{5/2}$ and Pt $4f_{7/2}$ excitations of metallic platinum, while the peaks with binding energies of 74.2 and 77.9 eV may be assigned to the Pt salt [21]. We conclude therefore, that more than 90% of platinum (II) acetylacetonate was reduced to elemental platinum during the pyrolysis of PAN nanofibers.

3.3. Electrocatalytic activity

The electrocatalytic activity of the Pt-CNFs for O_2 reduction was studied by RDE voltammetry. Fig. 5A shows the oxygen reduction hydrodynamic polarization scans in oxygen-purged 1 M sulfuric acid at different rotation rates; the background scan is from an argon-purged solution. The limiting electrocatalytic current plateau decreases with decreasing the rotation rate. Additionally, the curves shifted to a lower voltage after each scan suggesting that the electrode loses parts of its activity during each measurement. The electrocatalytic current of the three electrodes with the background subtracted is shown in Fig. 5B. It is obvious that the oxygen reduction happens at a much higher voltage (0.94 V relative to the reference electrode) for the Pt-CNFs electrode than either of the controls, the Pt-C (0.22 V) or the CNFs (0.28 V) electrode. Hence, the electrocatalytic activity comes from the Pt nanoparticles dispersed in the high surface-area CNFs. Given that the Ag/AgCl reference electrode (in 3 M NaCl) is 206 mV relative to normal hydrogen electrode, the Pt-CNFs electrode shows a better catalytic activity than the arrays of carbon nanotubes supporting high dispersion of Pt nanoparticles achieved by more complicated procedures [9]. In fact, the scan of the Pt-CNFs electrode is comparable to data from a pure Pt thin-film electrode [18].

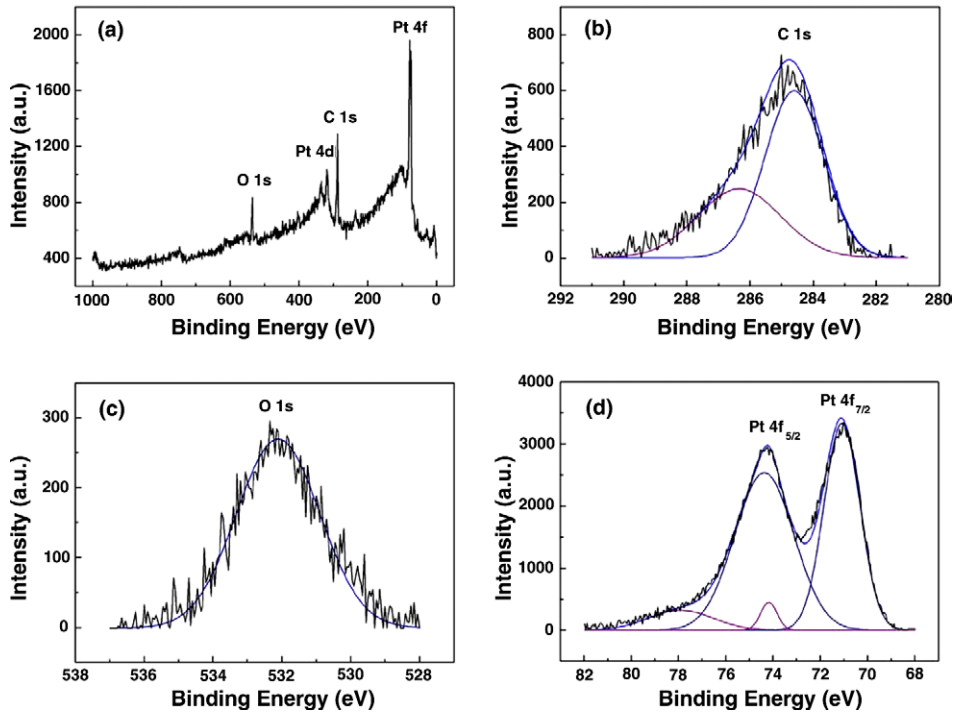

Fig. 4. (a) XPS survey spectrum of the Pt-CNFs; (b) C 1s (c) O 1s (d) Pt 4f XPS spectrums of the specimen.

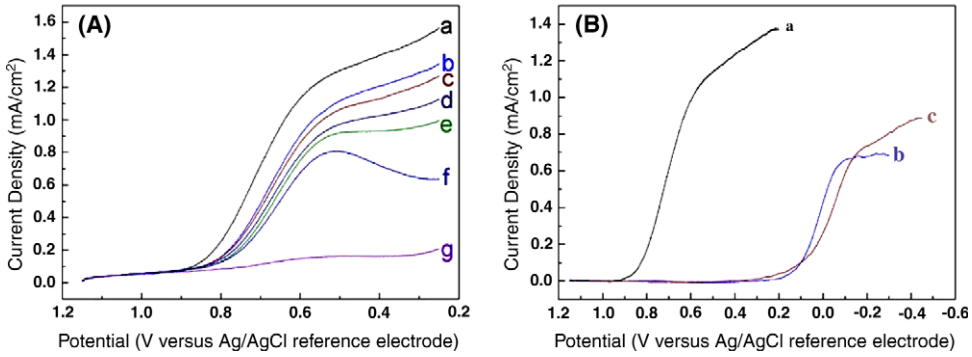

Fig. 5. (A) Oxygen reduction hydrodynamic polarization scans of Pt-CNFs electrodes in oxygen-purged 1 M sulfuric acid at different rotation rate (a, 1000 rpm; b, 800 rpm; c, 600 rpm; d, 400 rpm; e, 200 rpm; f, 0 rpm) and the background scan g in argon-purged electrolyte at 1000 rpm; (B) oxygen reduction hydrodynamic polarization scans of different electrodes (a, Pt-CNFs electrode; b, Pt-C electrode; c, CNFs electrode).

4. Conclusions

Porous AAO templates made by a two-step anodization of highly pure aluminum foil enable an in situ fabrication of hexagonally closed-packed PAN-based carbon nanofibers containing highly dispersed Pt nanoparticles. RDE voltammetry shows that this new composite material has a better electrocatalytic activity than similiar materials fabricated via more complicated procedures. Tests of Pt-CNFs for fuel cell applications are under way.

Acknowledgements

This work is supported by NASA University Research, Engineering and Technology Institute on Bio Inspired Materials (BIMAT) under award No. NCC-1-02037. The authors thank Dr. Srikanth Ranganathan, Dr. Qi Zhang, Aaron Rothrock, Dr. Hui Xu, and Dr. Wallace Ambrose for help during characterization. The authors also thank Professors Royce Murray and Zhibo Zhang, and Dr. Bin Wu for helpful discussions.

References

[1] S.H. Joo, S.J. Choi, I. Oh, J. Kwak, Z. Liu, O. Terasaki, R. Ryoo, Nature 412 (2001) 169.
[2] B. Rajesh, V. Karthik, S. Karthikeyan, K.R. Thampi, J.M. Bonard, B. Viswanathan, Fuel 81 (2002) 2177.
[3] C. Wang, M. Waje, X. Wang, J.M. Tang, R.C. Haddon, Y. Yan, Nano Lett. 4 (2004) 345.
[4] H. Tang, J. Chen, Z. Huang, D. Wang, Z. Ren, L. Nie, Y. Kuang, S. Yao, Carbon 42 (2004) 191.
[5] W.A. de Heer, A. Châtelain, D. Ugarte, Science 270 (1995) 1179.
[6] J. Kong, N.R. Franklin, C. Zhou, M.G. Chapline, S. Peng, K. Cho, H. Dai, Science 287 (2000) 622.
[7] C.R. Martin, Science 266 (1994) 1961.
[8] F. Li, L. Zhang, R.M. Metzger, Chem. Mater. 10 (1998) 2470.
[9] S.J. Shingubara, Nanoparticle Res. 5 (2003) 17.
[10] J.C. Hulteen, H.X. Chen, C.K. Chambliss, C.R. Martin, Nanostruct. Mater. 9 (1997) 133.
[11] S. Rahman, H. Yang, Nano Lett. 3 (2003) 439.
[12] H. Gao, C. Mu, F. Wang, D. Xu, K. Wu, Y. Xie, S. Liu, E. Wang, J. Xu, D.J. Yu, Appl. Phys. 93 (2003) 5602.
[13] H. Masuda, K. Fukuda, Science 268 (1995) 1466.
[14] O. Jessensky, F. Müller, U. Gösele, Appl. Phys. Lett. 72 (1998) 1173.
[15] H. Bu, J. Rong, Z. Yang, Macromol. Rapid Commun. 23 (2002) 460.
[16] T.T. Xu, R.D. Piner, R.S. Ruoff, Langmuir 19 (2003) 1443.
[17] B. Cheng, C.W. Murry, E.T. Samulski, Mater. Res. Soc. Symp. Proc. 737 (2003) 413.
[18] Z. Liu, J.Y. Lee, W. Chen, M. Han, L.M. Gan, Langmuir 20 (2004) 181.
[19] S. Ye, A.K. Vijh, L.H. Dao, J. Electrochem. Soc. 144 (1997) 90.
[20] J. Dai, M.L. Bruening, Nano Lett. 2 (2002) 497.
[21] J.A. Poirier, G.E. Stoner, J. Electrochem. Soc. 141 (1994) 425.